
Seasonal and multi-decadal zinc isotope variations in blue mussels from two sites with contrasting zinc contamination levels

Ferreira Araujo Daniel ^{1,*}, Ponzevera Emmanuel ¹, Jeong Hyeryeong ¹, Briant Nicolas ¹,
Le Monier Pauline ¹, Bruzac Sandrine ¹, Sireau Teddy ¹, Pellouin-Grouhel Anne ¹, Knoery Joël ¹,
Brach-Papa Christophe ²

¹ Ifremer, CCEM- Unité Contamination Chimique des Écosystèmes Marins, F-F-44300, Nantes, France

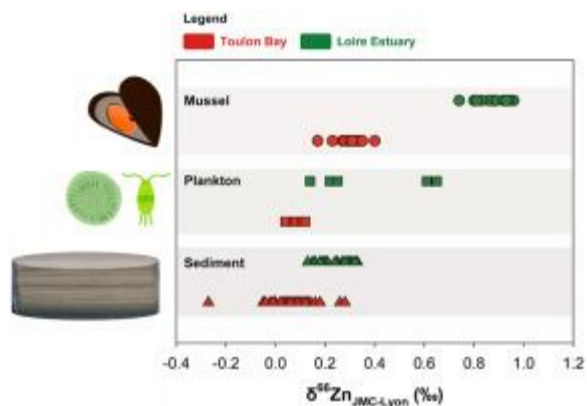
² Ifremer, LERPAC- Unité Littoral- Laboratoire Environnement Ressources Provence-Azur-Corse, F-83507, La Seyne-sur-Mer, France

* Corresponding author : Daniel Ferreira Araujo, email address : daniel.ferreira.araujo@ifremer.fr

Abstract :

Zinc (Zn) isotope compositions in soft mussel tissues help identify internal biological processes and track coastal Zn sources in coastal environments, thus aiding in managing marine metal pollution. This study investigated the seasonal and multi-decadal Zn isotope compositions of blue mussels (genus *Mytilus*) from two French coastal sites with contrasting Zn environmental contamination. Concurrently, we characterized the isotope ratios of sediments and plankton samples at each site to understand the associations between organisms and abiotic compartments. Our primary objective was to determine whether these isotope compositions trace long-term anthropogenic emission patterns or if they reflect short-term biological processes. The multi-decadal isotope profiles of mussels in the Loire Estuary and Toulon Bay showed no isotope variations, implying the enduring stability of the relative contributions of natural and anthropogenic Zn sources over time. At seasonal scales, Zn isotope ratios were also constant; hence, isotope effects related to spawning and body growth were not discernible. The multi-compartmental analysis between the sites revealed that Toulon Bay exhibits a remarkably lower Zn isotope ratio across all studied matrices, suggesting the upward transfer of anthropogenic Zn in the food web. In contrast, the Zn isotope variability observed for sediments and organisms from the Loire Estuary fell within the natural baseline of this element. In both sites, adsorptive geogenic material carrying significant amounts of Zn masks the biological isotope signature of plankton, making it difficult to determine whether the Zn isotope ratio in mussels solely reflects the planktonic diet or if it is further modified by biological homeostasis. In summary, Zn isotope ratios in mussels offer promising avenues for delineating source-specific isotope signatures, contingent upon a comprehensive understanding of the isotope fractionation processes associated with the trophic transfer of this element through the plankton.

Graphical abstract



Highlights

► Pristine and contaminated sites show samples with distinct isotope fingerprints. ► Systematic lighter $\delta^{66}\text{Zn}$ values identify anthropogenic Zn in contaminated samples. ► Zn isotopes trace upward transfer of anthropogenic Zn in the food web. ► Isotope biomonitoring indicates no alterations in Zn sources over four decades. ► Zn isotope ratio constancy at seasonal scale discards biological isotope effects.

Keywords : metal stable isotopes, isotope tracer, biomonitoring, marine pollution, trace metal bioaccumulation, zinc contamination

56

57 **1. Introduction**

58 Zinc (Zn) is a trace metal essential to life with a complex marine biogeochemical cycle
59 involving diverse processes (biological uptake, adsorption, ligand complexation, etc.) through
60 sediment, water, and biological interfaces (Rainbow, 2007). However, human activities have
61 disturbed its natural cycle by increasing Zn inputs in bioavailable forms into the marine
62 environment. These disruptions have led to the bioaccumulation of Zn in many marine species
63 at elevated levels, negatively impacting biota health and marine seafood quality (de Souza
64 Machado et al., 2016; Sen and Peucker-Ehrenbrink, 2012).

65 In nature, Zn primarily exists as five stable isotopes: ^{64}Zn , ^{66}Zn , ^{67}Zn , ^{68}Zn , and ^{70}Zn
66 (Moynier et al., 2017). These isotopes possess different atomic masses and form bonds with
67 varying quantum energies, resulting in their uneven distribution through biogeochemical
68 processes, and significant variability in isotope compositions across natural materials
69 (Wiederhold, 2015). These isotope compositions, expressed as the ratio between the
70 abundances of two isotopes, can change in time and space as they are modulated by different
71 factors such as geochemical sources, the reversibility of chemical processes, temperature,
72 coordination chemistry (geometry and bond length), and biological regulation (Albarede et al.,
73 2016; Andronikov et al., 2021; Aucour et al., 2015; Juillot et al., 2023; Komárek et al., 2021;
74 Sullivan et al., 2022; Wang et al., 2022). Thus, natural samples have their own Zn isotope
75 "fingerprints" that provide integrated information on the environmental trajectory of this metal,
76 including sources and the processes leading up to its uptake and bioaccumulation (Albarède et
77 al., 2011; Jaouen et al., 2018; McCormack et al., 2021; Schilling et al., 2021; Toubhans et al.,
78 2020).

79 Continuous analytical and methodological improvements in multicollector inductively
80 coupled plasma mass spectrometry (MC-ICP-MS) have facilitated the isotope characterization
81 of various marine matrices in diverse applications (Araújo et al., 2022b; Little et al., 2021,
82 2014). For example, the metal isotope compositions of marine sediments reflect source mixing
83 processes and can help verify records of anthropogenic sources, primary activities, and
84 sedimentary material mixing (Araújo et al., 2019b; Little et al., 2018, 2016; Zhang et al., 2018).
85 In addition, they can shed light on different feeding strategies for Zn uptake in deep-sea marine
86 sponges (i.e., Zn associated with dissolved *vs.* particulate phases; Hendry and Andersen, 2013).
87 Zn isotopes in marine carbonates and corals have shown promise for tracking metal pollution
88 and ancient seawater conditions in paleoceanography (Little et al., 2021; Liu et al., 2023; Xiao
89 et al., 2020; Zhang et al., 2022). Unicellular organisms, such as diatoms, have also been shown

90 to fractionate Zn isotopes depending on transport mechanisms across cell membranes via active
91 and passive mechanisms (John et al., 2007; Köbberich and Vance, 2019). These examples
92 underscore the capacity of Zn isotopes to provide insights regarding the metal itself and the
93 physiological mechanisms associated with its cellular transport and processes. Moreover, such
94 insights can be garnered across various levels of biological organization, from molecular
95 chemistry to unicellular organisms to populations of a particular species and ultimately to
96 complete ecosystems.

97 As a globally abundant bivalve group inhabiting marine environments, mussels have
98 been a staple in human seafood consumption for centuries (Beyer et al., 2017). Today, mussels
99 are a marine commodity, accounting for nearly one-third of all aquaculture products sold in the
100 European Union (FAO, 2024). Given that the majority (90%) of commercial marine bivalves,
101 including mussels, oysters, and clams, comes from aquaculture, the environmental quality and
102 sanitary conditions of coastal marine environments are critical to ensure sustainable aquaculture
103 practices (Wijsman et al., 2019). France is the third-largest European producer of mussels,
104 following Spain and Italy (Rodríguez-Rodríguez and Bande Ramudo, 2017). While regulations
105 on metal emissions have reduced metal release in coastal environments in developed countries,
106 new technological uses of metals and remobilization from legacy contaminated sediments
107 require constant monitoring (Barreira et al., 2024; Thibon et al., 2021; Thibon et al., 2021).

108 Mussels, like many other bivalves, feed on phytoplankton by pumping and filtering
109 large volumes of water over their ciliated gills; thus, they incorporate metals dissolved in the
110 water and through the ingestion of filtered particles (Gosling, 2015). Thus mussel "soft tissues"
111 are good biomarker of metal exposure, suitable for biomonitoring anthropogenic contamination
112 in aquatic systems (Cai and Wang, 2019; Goldberg, 1975; Krishnakumar et al., 2018; Lu and
113 Wang, 2018). Several mussel biomonitoring networks, the so-called "Mussel Watch Programs"
114 (MWP), have been implemented in North America, Europe, and Asia (Briand et al., 2023;
115 Briand et al., 2021b; Cantillo, 1998; Claisse, 1989; Cossa and Tabard, 2020; Couture et al.,
116 2010; Jeong et al., 2021b; Lu et al., 2020; Lu and Wang, 2018; Shiel et al., 2012; Wang et al.,
117 2022). The French MWP is a successful example of a perennial biomonitoring project that has
118 operated uninterrupted since the late 1970s, filling a substantial bivalve soft tissue sample bank
119 covering the country's shoreline. This sample collection is highly valuable to test new analytical
120 techniques, including "non-traditional" stable metal isotopes (Araújo et al., 2021b; Shiel et al.,
121 2013). Combined with isotope approaches, such environmental samples help reconstruct the
122 contributions of metal pollution sources or to infer environmental changes that impact marine
123 biota, especially in farm aquaculture under intense anthropic pressure from legacy
124 contamination (Araújo et al., 2021b; Barreira et al., 2024). Subsequent spatial analysis

125 conducted on mussels from the Korean coast show that they reflect the natural and
126 anthropogenic source apportionment of Zn in the surrounding environment (Jeong et al.,
127 2021b).

128 In this study, we investigated multi-decadal and seasonal variations in the Zn isotope
129 compositions of blue mussels (*Mytilus edulis* and *Mytilus galloprovincialis*) from two distinct
130 environmental locations in France, each characterized by unique pollution histories: the Loire
131 Estuary and Toulon Bay. Our primary objective was to determine whether these isotope
132 compositions trace long-term anthropogenic emission patterns or if they reflect short-term
133 biological processes. To achieve this, we contextualized mussel isotope patterns with those of
134 local sediments and plankton samples to evaluate Zn transfer mechanisms between the studied
135 compartments.

136

137 **2. Material and methods**

138 *2.1 Study sites*

139 The macrotidal Loire Estuary (~106 km long) is located on the Atlantic coast at the mouth of
140 the Loire River, a major European river with a mean annual water flow of ~900 m³ s⁻¹. The
141 well-mixed and highly turbid sedimentary plume of this estuary extends over a large part of the
142 northern Bay of Biscay continental shelf (Dulaquais et al., 2020; Waeles et al., 2004). The
143 maximum turbidity zone (MTZ) is about 20–50 km long and extends over the Bay of Biscay
144 continental shelf (Briant et al., 2021a; Jalón-Rojas et al., 2016). The Loire Estuary traverses an
145 industrialized and urbanized watershed that comprises the metropolitan areas of Nantes and
146 Saint-Nazaire with over 800,000 inhabitants (Coynel et al., 2016; Grosbois et al., 2012).
147 Concentrations of trace metals in sediments from the Loire Estuary and its nearby coastal
148 environment show an overall and significant decline in metal contaminant levels (lead [Pb], Zn,
149 and copper [Cu]), probably due to a drop in metal emission subsequent to deindustrialization
150 and emission regulations since the 1980s (Briant et al., 2024). There is also an apparent increase
151 in the relative importance of metals related to diffuse urban sources (Araújo et al., 2019b; Briant
152 et al., 2021a; Coynel et al., 2016).

153 Toulon Bay is an urbanized coastal ecosystem that has historically hosted naval
154 activities (ports and shipyards) and approximately 600,000 inhabitants (Tessier et al., 2011; Fig.
155 1). Two freshwater rivers—the Las and Eygoutier—discharge into Toulon Bay (Fig. 1). A dike
156 built in the 19th century divides Toulon into two sub-basins labeled the "Small Bay" (9.8 km²,
157 semi-enclosed inner basin) on the northwestern side and the "Large Bay" (42.2 km², outer basin)
158 on the southeastern part (Fig. 1). The Small Bay is bordered by continuous urbanized areas,
159 military zones, industries, recreational and commercial ports, and former shipyards (last one

160 closed in 1989). In the same zone at the Saint Lazareth site, shellfish farming developed at the
161 end of the 19th century. The Large Bay has a single military zone, small beaches, and tourist
162 ports.

163 In November 1942, the French Navy fleet was scuttled and 100 ships were destroyed
164 and sunk, mostly in the Small Bay (Grasset, 2011). The subsequent raising and treatment of the
165 wrecks resulted in strong polymetallic contamination of Cu, Zn, mercury (Hg), cadmium (Cd),
166 Pb, and other trace metals in the bay's sediment (Dang et al., 2015b; Tessier et al., 2011). As a
167 result, the concentrations of metals, including Cu and Zn, are extremely high in the Small Bay.
168 Despite the low hydrodynamic energy that preserves the sedimentary stratum and its legacy of
169 anthropogenic metals, resuspension events in its shallow zone can mix contemporary and
170 legacy sedimentary metals (Araújo et al., 2019a; Pougnet et al., 2014). Indeed, sediment cores
171 reveal that the extreme Zn contamination associated with warfare materials and fleet scuttling
172 has shown only a minor decrease in metal levels in the sedimentary layers since the post-WWII
173 period (Tessier et al., 2011).

174

175 *2.2 Mussel sampling*

176 The preserved tissue samples of mussels used in this study were obtained from bank samples
177 collected through the French National Monitoring Network 'ROCCH' (Observation Network of
178 Chemical Contamination of the Marine Environment), managed by Ifremer (the French
179 Research Institute for Exploitation of the Sea). The mussel samples selected for this study were
180 obtained from the Chemoulin site in the Loire Estuary and the Saint Lazaret site in Toulon Bay
181 (Fig. 1). The Chemoulin site near the Loire Estuary mouth constitutes a beach system with a
182 coarse deposition of sand grains via high hydrodynamic energy from the sea. The Saint Lazaret
183 site, located in inner Toulon Bay (Small Bay), has very low hydrodynamic energy, possesses a
184 shallow water column (~9m) where high load of fine sediments are often resuspended from the
185 bottom sediments due to seawater currents and intense navy boat traffic.

186 Two collections of mussel samples spanning four decades of biomonitoring from the
187 early 1980s to the end of the 2010s, were selected from the Loire Estuary (Chemoulin site) and
188 Toulon Bay (Saint Lazaret site), respectively. These multi-decadal bivalve series used samples
189 collected in the same season (autumn) to minimize the potential influence of seasonally varying
190 parameters, such as the organism's spawning cycle, primary production, water biomass, and
191 continental runoff fluxes. Two other collections of mussels from Chemoulin and Saint Lazaret
192 sites representing an entire seasonal period (winter-spring-summer-autumn) in 1997 was also
193 included.

194 All mussels samples followed the same sampling and chemical preparation protocols
195 (Grouhel, 2023). Briefly, these bivalve mollusks were harvested from beach rocks (Loire
196 Estuary) or aquaculture cages (Toulon Bay) and transported to the laboratory, where they were
197 kept in local seawater for 24 hours to depurate. Each sample represented a pool of at least 50
198 mussels that were crushed, homogenized, and freeze-dried.

199

200 *2.3 Plankton*

201 Plankton samples were collected were collected using a polymeric cod-end attached to a
202 plankton net with circular openings of 0.25 m² and a mesh size of 63 µm. The net opening was
203 pulled horizontally at a depth of 5 m below the water surface at a speed of 0.2–1.0 knots. The
204 plankton size fractions were obtained by filtering the contents of the plankton net's cod-end
205 through a vertical array of nylon sieves with decreasing mesh sizes (from 1000 to 63 µm) to
206 obtain three plankton size classes: 1000-500 µm, 500-250 µm, and 250-63 µm. For each sieve,
207 the plankton fraction was collected in acid-cleaned polyethylene tubes, frozen, freeze-dried,
208 and stored for later analysis. Sampling in the Loire Estuary dates back to the spring of 2013 at
209 two stations (LE1 and LE2), and in Toulon Bay, it took place during the spring and autumn of
210 2018 at two stations (TB1 and TB2). For LE2 station, the 500-1000 µm particle-size class is
211 missing due to insufficient material for chemical analysis.

212

213 *2.4 Sediments*

214 In the Loire Estuary 17 surface sediments (0-5 cm) collected in 2014 using an Ekman and
215 Reineck crabs were acquired from the sample bank of the ROCCH monitoring framework. In
216 addition, a sediment core labeled "PV1" (300 cm length) was sampled on the inner intertidal
217 mudflat of the Loire Estuary (Fig. 1) during the Paleovase mission in March 2015. The coring
218 used aluminum tubes (6 m long, 74 mm internal diameter, and 1 mm wall), and, was then
219 subsampled into 2-cm-thick sediment slices every 5 cm in the upper meter, and every 10 cm
220 for the rest of the sediment core. The ²¹⁰Pb dating technique and geochemical metal
221 concentration profiles enabled us to infer the commencement of the postindustrialization period
222 at a depth of 96 cm in the PV1 core, corresponding to approximately the end of the 19th century
223 (Araújo et al., 2021b). In Toulon Bay, 52 sampling sites of surface sediment (0–5 cm) were
224 collected between November 2008 and June 2009 within the framework of the CARTOCHIM
225 project (Fig. 1).

226

227 *2.5 Sample preparation and chemical analysis*

228 Approximately 200 mg of dry bivalve tissue samples were digested using an HNO₃ solution
 229 (50% v/v) in a microwave (MARS 5, CEM®). Dry aliquots of sediments were digested in
 230 Teflon® bombs on a Teflon-coated graphite block using multistep additions of high-quality
 231 concentrated HF, HCl, and HNO₃ for trace metal analysis. Plankton samples were prepared by
 232 following the same protocol as sediments but without HF. Aliquots were taken from final
 233 digestion solutions for subsequent elemental and isotope analysis. To ensure accuracy,
 234 procedural blanks and certified reference materials were processed in each batch of sediment
 235 samples following all procedures (digestion, elemental analysis, ion-exchange chromatography,
 236 and isotope determination). Certified reference materials included oyster and mussel tissues
 237 (SRM 1566b;NIST®, and ERM-CE278k;ERM®), plankton (BCR-414) and sediments (MESS-
 238 3 and PACS-2 from NRC – CNR®).

239 Elemental Zn was measured by ICP-MS (iCAP, Thermo Scientific), and isotope
 240 analyses were conducted using Multicollector (MC-)ICP-MS (Neptune, Thermo Scientific) at
 241 the PSO platform (Pôle Spectrométrie Océan, Ifremer, France). The measured Zn
 242 concentrations aligned with the certified value of the reference material within ±10%. Isotope
 243 sample runs followed the standard bracketing mode combined with external normalization (Cu-
 244 doping). The final Zn isotope compositions are expressed using δ-notation as follows:

245

$$246 \quad \delta^{66/64}\text{Zn}_{JMC-Lyon} (\text{‰}) = \left(\frac{R\left(\frac{66\text{Zn}}{64\text{Zn}}\right)_{\text{sample}}}{R\left(\frac{66\text{Zn}}{64\text{Zn}}\right)_{JMC-Lyon}} - 1 \right) \times 1000 \quad (\text{Eq. 1})$$

247

248 To ensure analytical quality control, reference materials of bivalve mollusk tissues, plankton,
 249 and sediments were measured at least two times during each analytical session. The average
 250 values for δ⁶⁶Zn_{JMC-Lyon} are reported in Table 1. The precision of a given sample measure was
 251 two standard deviations (2s) and commonly below 0.1‰. All reagents, labware cleaning, and
 252 solution dilutions for elemental and isotope analyses were performed using 18.2 MΩ cm H₂O
 253 (Nanop System®) and high-purity acids (PlasmaPure Plus grade, SCP science®).

254

255 **3. Result and discussions**

256 *3.1 Zinc datasets summary*

257 Table 2 summarize all data utilized in the present study, encompassing both newly collected
 258 information and compiled data. The plankton data samples from the Loire Estuary were
 259 compiled from a prior study (Araújo et al., 2022a) and can be found in Table S1 (Supplementary

260 Material). Additionally, new plankton data from Toulon Bay are presented this study (Table
261 S1). All bottom sediment data were compiled from previously published studies in Toulon Bay
262 (Araújo et al., 2019a) and in the Loire Estuary (Araújo et al., 2019b), which are detailed in
263 Tables S2 and S3. All mussel isotope data presented here is summarized in the Table S4.

264

265 3.2 Elemental and isotope profiles of Zn in mussels at seasonal scale

266 Both the Loire Estuary and Toulon Bay showed similar seasonal patterns of Zn
267 bioaccumulation, with mussels having higher Zn concentrations in winter and lower levels in
268 summer (Fig. 2). In contrast, the Zn isotope profile in mussel populations of both sites remained
269 seasonally constant over the 1-year biomonitoring period (1997), around $+0.89 \pm 0.05$ (n = 4,
270 2s) and $+0.27 \pm 0.05\text{‰}$ (n = 4, 2s), for the Atlantic and Mediterranean sites, respectively. The
271 detailed isotope dataset for mussel samples are included in Table S4.

272 The seasonal growth and reproductive cycle of mussels strongly influence their
273 bioaccumulation of trace metals at a seasonal scale. *Mytilus* mussels become sexually mature
274 after 1–2 years and tend to spawn in the spring, synchronizing with the main phytoplankton
275 bloom in spring (Beyer et al., 2017). During cold periods (winter and early spring), energy
276 requirements, gonadal development, and gametogenesis increase, leading to higher
277 bioaccumulation of trace metals such as Cu and Zn (Azizi et al., 2018; Benali et al., 2015; Soto
278 et al., 2000). The highest Zn concentrations in the winter samples align with this expected trend.
279 However, it is worth noting that this increase can coincide with anthropogenic inputs via runoff
280 triggered by rainy French winters (Nicolau et al., 2012; Oursel et al., 2014; Schlacher-
281 Hoenlinger and Schlacher, 1998).

282 In spring, mussel body growth increases with food availability, leading to a biodilution
283 of metal concentrations (Azizi, 2018). In the subsequent spawning period (later spring and
284 summer), the emission of gametes can significantly decrease mussel biomass and metal
285 contents (Adami et al., 2002; Azizi et al., 2018). The timing of *Mytilus* population spawning
286 varies greatly with geographic location (Latouche and Mix, 1981; Lobel and Wright, 1982).
287 The Zn concentrations in Loire Estuary mussels showed drastic concentration decreases of
288 almost 50% between winter and spring, which seems unlikely to be restricted to biodilution
289 effects. We suggest that these mussels start the spawning period earlier, in spring, compared
290 with bivalves from Toulon Bay, which have a summer spawning period. Therefore, organism
291 growth and reproduction cycles likely explain the decreased Cu and Zn concentrations in spring,
292 with the lowest values in summer.

293 In contrast to elemental data, a constant seasonal Zn isotope profile indicates that body
294 growth and reproductive cycles do not affect the isotope compositions of soft tissues. It is well

295 known that Zn coordination changes can trigger isotope fractionation through transport,
296 compartmentalization, detoxification, and excretion in living organisms (Balter et al., 2010;
297 Caldelas et al., 2011; Caldelas and Weiss, 2017; Moynier et al., 2020). We can then hypothesize
298 that internal cellular Zn trafficking modulated by ligands with similar electron donors, such as
299 metallothionein proteins (S-donors), leads to similar Zn speciation among cellular and tissue
300 Zn pools, resulting in a negligible isotope fractionation during spawning processes.

301

302 *3.3 Elemental and isotope profiles of Zn in mussels over decades*

303 The Zn isotope compositions in mussels from both sites have remained almost constant during
304 several decades (Fig. 3). In the Loire Estuary, mussels have $\delta^{66}\text{Zn}_{\text{JMC-Lyon}}$ values ranging from
305 approximately +0.7‰ to +0.9‰ and concentrations around $135 \pm 77 \mu\text{g g}^{-1}$ ($n = 10, 2s$). Toulon
306 Bay mussels have lighter $\delta^{66}\text{Zn}_{\text{JMC-Lyon}}$ values, falling in the range of +0.2‰ to +0.4‰, and
307 relatively higher concentrations with an average of $180 \pm 97 \mu\text{g g}^{-1}$ ($n = 14, 2s$). The lack of
308 discernible temporal trends in elemental and isotope Zn patterns complicates the attribution of
309 isotope shifts to changes in source apportionment. Nevertheless, the remarkable disparity in
310 isotope signatures among sampling stations stands out. In subsequent sections, we employ
311 sediment data to contextualize natural and anthropogenic Zn sources. Additionally, we explore
312 the roles of plankton size classes in the trophic Zn transfer to explain the observed spatial
313 differences.

314

315 *3.4 Zn systematics in sediments*

316 Metal concentrations in sediments are susceptible to grain-size distributions, especially when
317 comparing sediments from different geological settings. Given the acknowledged significance
318 of analyzing finer fractions in the assessment of trace metals, which demonstrate a high affinity
319 for adsorption onto clay minerals and Fe and Mn-oxyhydroxides, we opted in this study to use
320 aluminum (Al) as a proxy for the clay fraction content and to normalize concentrations based
321 on 5% of this element (Kersten and Smedes, 2002; OSPAR, 2018). Consequently, normalized
322 Zn concentrations in sediments are used henceforth in the following discussion

323 In the Loire Estuary, surface and core sediments display low to moderate Zn
324 concentrations varying between 43 and $157 \mu\text{g g}^{-1}$, an overall average of $116 \pm 28 \mu\text{g g}^{-1}$ ($n =$
325 $32, 1s$, Fig. 4) (Fig. 4). The Zn isotope compositions of sediments are relatively homogeneous
326 (Fig. 4), with $\delta^{66}\text{Zn}_{\text{JMC-Lyon}}$ averaging $+0.24\text{‰} \pm 0.11\text{‰}$ ($2s, n = 26$) (Fig. 4). Most $\delta^{66}\text{Zn}_{\text{JMC-}}$
327 Lyon values of Loire sediment fall within the crustal range, indicating dominance of geogenic
328 Zn. This pattern seems consistent considering Zn concentrations are close to the natural
329 background estimated at $90 \mu\text{g g}^{-1}$ to the North-East Atlantic coast (OSPAR, 2018). Some

330 samples with Zn concentrations above $100 \mu\text{g g}^{-1}$ fall outside the geogenic isotope range, likely
331 indicating a minor influence of anthropogenic sources. Overall, anthropogenic urban Zn sources
332 tend to have lighter $\delta^{66}\text{Zn}_{\text{JMC}}$ values than the geological background, such as tire wear (from
333 $+0.00\text{‰}$ to $+0.20\text{‰}$), gasoline (from -0.50‰ to $+0.07\text{‰}$), urban runoff (from $+0.13\text{‰}$ to
334 $+0.15\text{‰}$), wastewaters and sludge ($\sim 0.05\text{‰}$), industrial effluents (chemical and agro-food
335 industry, from $+0.10\text{‰}$ to $+0.15\text{‰}$), and atmospheric industrial emissions (from -0.6‰ to
336 $+0.15\text{‰}$). A detailed compilation of Zn sources for aquatic systems can be found in Desaulty
337 and Petelet-Giraud, (2020). Nevertheless, the relatively close values between natural (~ 0.3)
338 and anthropogenic Zn (~ 0.1), along with the low degree of Zn enrichment in the investigated
339 samples, make it challenging to precisely define and compute the anthropogenic Zn's relative
340 influence.

341 In turn, the levels of Zn contamination in Toulon's Small and Large Bays show a
342 remarkable contrast (Fig. 4). In the Small Bay, sediments are highly enriched in Zn, averaging
343 around $387 \pm 320 \mu\text{g g}^{-1}$ ($n = 24$, 1s), while in the Large Bay, Zn concentrations remain mostly
344 within $125 \pm 55 \mu\text{g g}^{-1}$ ($n = 28$, 1s). Nevertheless, Zn isotope compositions in the Small and
345 Large Bays have identical averages: $+0.06\text{‰} \pm 0.05\text{‰}$ (1s, $n = 24$) and $+0.06\text{‰} \pm 0.11\text{‰}$ ($n =$
346 28 , 1s), respectively (Fig. 4). Similarly, the spatial distribution of Pb isotopes in surface
347 sediments are relatively homogeneous between the two sub-bays, despite higher Pb
348 contamination levels in Small Bay (Dang et al., 2015b). The consistent spatial isotope
349 distribution pattern of Zn and Pb may be attributed to the significant export of anthropogenic
350 Zn from the inner bay toward the open sea. Thus, the mussel sampling station located in the
351 Small Bay, with an overwhelming dominance of anthropogenic Zn, provides an opportunity to
352 test whether anthropogenic isotope signals from the mussel's environment can be transduced
353 into mussel tissues or whether they remain traceable after isotope fractionation by
354 biogeochemical processes.

355

356 *3.5 Zn systematics in plankton*

357 The plankton from Toulon Bay exhibit greater isotope homogeneity across different plankton
358 sizes (Fig. 5a), with $\delta^{66}\text{Zn}_{\text{JMC-Lyon}}$ values displaying a remarkably consistent range of around
359 $+0.08\text{‰} \pm 0.06\text{‰}$ ($n = 9$, 2s). We found no significant spring-to-summer change in the Zn
360 isotope compositions (average $\Delta^{66}\text{Zn}_{\text{spring-summer}} = -0.01\text{‰}$). Spatial comparison between sites
361 located in the Small and Large bays from Toulon Bay (TB1 vs. TB2) were very similar (Fig.
362 5a). Zinc concentrations vary between 95 and $264 \mu\text{g g}^{-1}$ (Table S1), and are uncorrelated to
363 isotope ratios. Comparatively, the observed $\delta^{66}\text{Zn}_{\text{JMC-Lyon}}$ values in plankton sub-fractions from
364 the Loire Estuary display a broader range, from $+0.14$ to $+0.76\text{‰}$ (Fig. 5a) and lower Zn

365 concentration levels, with minimum and maximum of 66 to 199 $\mu\text{g g}^{-1}$, respectively (Table S1).
366 The LE2 stations stand out with the larger plankton sizes showing more positive isotope ratios.
367 These two samples also accompany the lowest Al contents (Fig. 5b).

368 Geogenic particles carrying substantial amounts of Zn can obscure the biogenic Zn
369 signal. Utilizing Al and iron (Fe) as proxies for terrigenous materials allows us to observe a
370 considerable presence of geogenic material in plankton samples (Fig S1). Consequently, the
371 close isotope values between some plankton size classes and sediments observed at the two
372 sites are likely related to the contamination of geogenic particles in plankton (Fig. 6). A survey
373 on Mediterranean plankton has demonstrated a tendency for plankton samples associated with
374 geogenic particles to enrich in Zn lighter isotopes (Chifflet et al., 2022). In Toulon Bay, the
375 homogeneity of Zn isotope composition is likely explained by the resuspension of sediment
376 particles from the seafloor. This process increases the abundance of geogenic materials in
377 Toulon Bay's shallow water column, masking the small biogenic fraction of the seston. In the
378 Loire Estuary, the balance between geogenic and biogenic pools can vary based on the
379 hydrodynamic particle sorting along the estuary's sediment plume dispersion (Araújo et al.,
380 2022a). Nevertheless, we infer that the low Al contents in the two exceptional samples from the
381 Loire Estuary (LE2 station, 250-500 and 500-1000 μm) suggest minimal geogenic material,
382 indicating biogenic Zn dominance. Notably, these two samples exhibit isotope ratios more in
383 line with those of mussels from the Loire Estuary, even though they do not overlap (Fig. 6).

384

385 *3.6 Multi-compartmental Zn isotope analysis: summary and final considerations*

386 Multi-compartmental Zn isotope patterns reveal a distinct trend toward a lighter isotope
387 composition for sediment, plankton, and mussels from Toulon Bay compared with the Loire
388 Estuary (Fig. 6). In Toulon Bay, we identified this light isotope signature in sediments as
389 anthropogenic. The high contents of geogenic elements (Al and Fe) in plankton samples
390 indicate an important fraction of mineral material. Thus, the close values between plankton and
391 surface sediments are likely a result of sediment particle resuspension from the bottom to the
392 water column in this shallower area of the inner bay. Consequently, the obscured isotope signals
393 of the 'true plankton fraction contribute to uncertainty in understanding whether the observed
394 isotope offset in *Mytillus galloprovincialis* at this site stems from a possible biological isotope
395 fractionation process related to the internal Zn regulation. In the Loire Estuary, sediments
396 mostly fall in the natural isotope range of Zn for coastal sediments. The plankton of different
397 size classes exhibits varying isotope variability. However, as noted for Toulon Bay, the isotope
398 signal of the biogenic fraction can be masked depending on the relative presence of geogenic
399 material (Araújo et al., 2022a). The heavy Zn isotope ratio for biogenic particles (identified

400 here with low Al contents, Fig. 5b) falls close to the isotope range of mussels. Nevertheless,
401 conducting additional plankton sampling in the vicinity of bivalve mollusks could enhance the
402 precision of the analysis of biogenic Zn pools.

403 The presented multi-compartmental analysis shows thus that understanding the isotope
404 composition of plankton is crucial for a more nuanced comprehension of Zn food-web transfers
405 and the associated isotope fractionation. Mussels species have physiologies adapted to feed on
406 specific plankton communities that vary in size and Zn contents (Gosling, 2015). Therefore, it
407 becomes imperative to conduct isotope analyses targeting specific plankton fractions that
408 constitute the specific diets for each species. However, the inherent mineral "contamination" of
409 plankton sampling in turbid coastal environments makes determining its specific isotope
410 compositions analytically challenging. As a result, establishing elusive isotope baselines for the
411 marine food web remains a significant challenge. The temporal isotope profiles of mussels over
412 multi-decadal periods remain relatively constant in both the Loire Estuary and Toulon Bay,
413 suggesting that the relative contributions of natural and anthropogenic Zn sources have
414 remained unchanged. In contrast, in the Loire Estuary, natural zinc is expected to be more
415 dominant. Building upon previous studies, we posit that anthropogenic zinc is likely strongly
416 associated with suspended particles and susceptible to exchange with biotic interfaces (Dang et
417 al., 2015a; Tessier et al., 2011). Thus, we conclude that the elevated concentration of
418 anthropogenic Zn in Toulon Bay has moved up in the food web, bringing lighter isotope ratios
419 in the mussels.

420 At short seasonal scales, internal biological isotope fractionation linked to spawning and
421 body growth does not significantly affect Zn isotope ratios over seasons. Given the consistent
422 Zn isotope ratios in mussels throughout seasonal and multi-decadal scales, they can offer
423 potential avenues for delineating source-specific isotope signatures, contingent upon
424 understanding the isotope fractionation related to the trophic transfer of Zn via plankton diets.

425

426 **Acknowledgments**

427 The authors thank the Pays de La Loire and Provence-Alpes-Côte d'Azur for funding the
428 POLLUSOLS and SCOTTI projects.

429

430 **References**

- 431 Adami, G., Barbieri, P., Fabiani, M., Piselli, S., Predonzani, S., Reisenhofer, E., 2002. Levels of
432 cadmium and zinc in hepatopancreas of reared *Mytilus galloprovincialis* from the Gulf of
433 Trieste (Italy). *Chemosphere* 48, 671–677. [https://doi.org/10.1016/S0045-6535\(02\)00196-0](https://doi.org/10.1016/S0045-6535(02)00196-0)
434 Albarede, F., Télouk, P., Balter, V., Bondanese, V.P., Albalat, E., Oger, P., Bonaventura, P., Miossec,
435 P., Fujii, T., 2016. Medical applications of Cu, Zn, and S isotope effects. *Metallomics* 8, 1056–
436 1070. <https://doi.org/10.1039/C5MT00316D>

- 437 Albarède, F., Telouk, P., Lamboux, A., Jaouen, K., Balter, V., 2011. Isotopic evidence of unaccounted
438 for Fe and Cu erythropoietic pathways. *Metallomics* 3, 926. <https://doi.org/10.1039/c1mt00025j>
- 439 Andronikov, A.V., Novak, M., Oulehle, F., Chrastny, V., Sebek, O., Andronikova, I.E., Stepanova, M.,
440 Sipkova, A., Hruska, J., Myska, O., Chuman, T., Veselovsky, F., Curik, J., Prechova, E.,
441 Komarek, A., 2021. Catchment Runoff in Industrial Areas Exports Legacy Pollutant Zinc from
442 the Topsoil Rather than Geogenic Zn. *Environ. Sci. Technol.* 55, 8035–8044.
443 <https://doi.org/10.1021/acs.est.1c01167>
- 444 Araújo, D., Machado, W., Weiss, D., Mulholland, D.S., Boaventura, G.R., Viers, J., Garnier, J., Dantas,
445 E.L., Babinski, M., 2017. A critical examination of the possible application of zinc stable
446 isotope ratios in bivalve mollusks and suspended particulate matter to trace zinc pollution in a
447 tropical estuary. *Environmental Pollution* 226, 41–47.
448 <https://doi.org/10.1016/j.envpol.2017.04.011>
- 449 Araújo, D.F., Knoery, J., Briant, N., Ponzevera, E., Chouvelon, T., Auby, I., Yopez, S., Bruzac, S.,
450 Sireau, T., Pellouin-Grouhel, A., Akcha, F., 2021a. Metal stable isotopes in transplanted oysters
451 as a new tool for monitoring anthropogenic metal bioaccumulation in marine environments: The
452 case for copper. *Environmental Pollution* 290, 118012.
453 <https://doi.org/10.1016/j.envpol.2021.118012>
- 454 Araújo, D.F., Knoery, J., Briant, N., Ponzevera, E., Mulholland, D.S., Bruzac, S., Sireau, T., Chouvelon,
455 T., Brach-Papa, C., 2022a. Cu and Zn stable isotopes in suspended particulate matter sub-
456 fractions from the Northern Bay of Biscay help identify biogenic and geogenic particle pools.
457 *Continental Shelf Research* 104791. <https://doi.org/10.1016/j.csr.2022.104791>
- 458 Araújo, D.F., Knoery, J., Briant, N., Vigier, N., Ponzevera, E., 2022b. “Non-traditional” stable isotopes
459 applied to the study of trace metal contaminants in anthropized marine environments. *Marine*
460 *Pollution Bulletin* 175, 113398. <https://doi.org/10.1016/j.marpolbul.2022.113398>
- 461 Araújo, D.F., Ponzevera, E., Briant, N., Knoery, J., Bruzac, S., Sireau, T., Brach-Papa, C., 2019a.
462 Copper, zinc and lead isotope signatures of sediments from a mediterranean coastal bay
463 impacted by naval activities and urban sources. *Applied Geochemistry* 111, 104440.
464 <https://doi.org/10.1016/j.apgeochem.2019.104440>
- 465 Araújo, D.F., Ponzevera, E., Briant, N., Knoery, J., Sireau, T., Mojtahid, M., Metzger, E., Brach-Papa,
466 C., 2019b. Assessment of the metal contamination evolution in the Loire estuary using Cu and
467 Zn stable isotopes and geochemical data in sediments. *Marine Pollution Bulletin* 143, 12–23.
468 <https://doi.org/10.1016/j.marpolbul.2019.04.034>
- 469 Araújo, D.F., Ponzevera, E., Weiss, D.J., Knoery, J., Briant, N., Yopez, S., Bruzac, S., Sireau, T., Brach-
470 Papa, C., 2021b. Application of Zn Isotope Compositions in Oysters to Monitor and Quantify
471 Anthropogenic Zn Bioaccumulation in Marine Environments over Four Decades: A “Mussel
472 Watch Program” Upgrade. *ACS EST Water* 1, 1035–1046.
473 <https://doi.org/10.1021/acsestwater.1c00010>
- 474 Aucour, A.-M., Bedell, J.-P., Queyron, M., Magnin, V., Testemale, D., Sarret, G., 2015. Dynamics of
475 Zn in an urban wetland soil–plant system: Coupling isotopic and EXAFS approaches.
476 *Geochimica et Cosmochimica Acta* 160, 55–69. <https://doi.org/10.1016/j.gca.2015.03.040>
- 477 Azizi, G., 2018. The use of *Mytilus* spp. mussels as bioindicators of heavy metal pollution in the coastal
478 environment. *Journal of Materials Science & Technology* 9(4), 1170–1181.
- 479 Azizi, G., Layachi, M., Akodad, M., Yáñez-Ruiz, D.R., Martín-García, A.I., Baghour, M., Mesfioui, A.,
480 Skalli, A., Moumen, A., 2018. Seasonal variations of heavy metals content in mussels (*Mytilus*
481 *galloprovincialis*) from Cala Iris offshore (Northern Morocco). *Marine Pollution Bulletin* 137,
482 688–694. <https://doi.org/10.1016/j.marpolbul.2018.06.052>
- 483 Balter, V., Zazzo, A., Moloney, A.P., Moynier, F., Schmidt, O., Monahan, F.J., Albarède, F., 2010.
484 Bodily variability of zinc natural isotope abundances in sheep. *Rapid Commun. Mass Spectrom.*
485 24, 605–612. <https://doi.org/10.1002/rcm.4425>
- 486 Barreira, J., Araújo, D.F., Knoery, J., Briant, N., Machado, W., Grouhel-Pellouin, A., 2024. The French
487 Mussel Watch Program reveals the attenuation of coastal lead contamination over four decades.
488 *Marine Pollution Bulletin* 199, 115975. <https://doi.org/10.1016/j.marpolbul.2023.115975>
- 489 Benali, I., Boutiba, Z., Merabet, A., Chèvre, N., 2015. Integrated use of biomarkers and condition indices
490 in mussels (*Mytilus galloprovincialis*) for monitoring pollution and development of biomarker
491 index to assess the potential toxic of coastal sites. *Marine Pollution Bulletin* 95, 385–394.
492 <https://doi.org/10.1016/j.marpolbul.2015.03.041>

- 493 Beyer, J., Green, N.W., Brooks, S., Allan, I.J., Ruus, A., Gomes, T., Bråte, I.L.N., Schøyen, M., 2017.
494 Blue mussels (*Mytilus edulis* spp.) as sentinel organisms in coastal pollution monitoring: A
495 review. *Marine Environmental Research* 130, 338–365.
496 <https://doi.org/10.1016/j.marenvres.2017.07.024>
- 497 Briand, M.J., Herlory, O., Briant, N., Brach-Papa, C., Boissery, P., Bouchoucha, M., 2023. The French
498 Mussel Watch: More than two decades of chemical contamination survey in Mediterranean
499 coastal waters. *Marine Pollution Bulletin* 191, 114901.
500 <https://doi.org/10.1016/j.marpolbul.2023.114901>
- 501 Briant, N., Chiffolleau, J.-F., Knoery, J., Araújo, D.F., Ponzevera, E., Crochet, S., Thomas, B., Brach-
502 Papa, C., 2021a. Seasonal trace metal distribution, partition and fluxes in the temperate
503 macrotidal Loire Estuary (France). *Estuarine, Coastal and Shelf Science* 262, 107616.
504 <https://doi.org/10.1016/j.ecss.2021.107616>
- 505 Briant, N., Knoery, J., Araújo, D.F., Ponzevera, E., Chauvelon, T., Bruzac, S., Sireau, T., Thomas, B.,
506 Mojtahid, M., Metzger, E., Brach-Papa, C., 2024. Vanishing lead in the Loire River estuary: An
507 example of successful environmental regulation. *Environmental Pollution* 340, 122860.
508 <https://doi.org/10.1016/j.envpol.2023.122860>
- 509 Briant, N., Le Monier, P., Bruzac, S., Sireau, T., Araújo, D.F., Grouhel, A., 2021b. Rare Earth Element
510 in Bivalves' Soft Tissues of French Metropolitan Coasts: Spatial and Temporal Distribution.
511 *Arch Environ Contam Toxicol*. <https://doi.org/10.1007/s00244-021-00821-7>
- 512 Cai, C., Wang, W.-X., 2019. Inter-species difference of copper accumulation in three species of marine
513 mussels: Implication for biomonitoring. *Science of The Total Environment* 692, 1029–1036.
514 <https://doi.org/10.1016/j.scitotenv.2019.07.298>
- 515 Caldelas, C., Dong, S., Araus, J.L., Jakob Weiss, D., 2011. Zinc isotopic fractionation in *Phragmites*
516 *australis* in response to toxic levels of zinc. *Journal of Experimental Botany* 62, 2169–2178.
517 <https://doi.org/10.1093/jxb/erq414>
- 518 Caldelas, C., Weiss, D.J., 2017. Zinc Homeostasis and isotopic fractionation in plants: a review. *Plant*
519 *Soil* 411, 17–46. <https://doi.org/10.1007/s11104-016-3146-0>
- 520 Cantillo, A. Y., 1998. Comparison of results of Mussel Watch Programs of the United States and France
521 with Worldwide Mussel Watch Studies. *Marine Pollution Bulletin* 36, 712–717.
522 [https://doi.org/10.1016/S0025-326X\(98\)00049-6](https://doi.org/10.1016/S0025-326X(98)00049-6)
- 523 Chifflet, S., Briant, N., Freyrier, R., Araújo, D.F., Quéméneur, M., Zouch, H., Bellaaj-Zouari, A.,
524 Carlotti, F., Tedetti, M., 2022. Isotopic compositions of copper and zinc in plankton from the
525 Mediterranean Sea (MERITE-HIPPOCAMPE campaign): Tracing trophic transfer and
526 geogenic inputs. *Marine Pollution Bulletin* 185, 114315.
527 <https://doi.org/10.1016/j.marpolbul.2022.114315>
- 528 Claisse, D., 1989. Chemical contamination of French coasts: The Results of a Ten Years Mussel Watch.
529 *Marine Pollution Bulletin* 20, 523–528. [https://doi.org/10.1016/0025-326X\(89\)90141-0](https://doi.org/10.1016/0025-326X(89)90141-0)
- 530 Cossa, D., Tabard, A.-M., 2020. Mercury in Marine Mussels from the St. Lawrence Estuary and Gulf
531 (Canada): A Mussel Watch Survey Revisited after 40 Years. *Applied Sciences* 10, 7556.
532 <https://doi.org/10.3390/app10217556>
- 533 Couture, R.-M., Chiffolleau, J.-F., Auger, D., Claisse, D., Gobeil, C., Cossa, D., 2010. Seasonal and
534 Decadal Variations in Lead Sources to Eastern North Atlantic Mussels. *Environ. Sci. Technol.*
535 44, 1211–1216. <https://doi.org/10.1021/es902352z>
- 536 Coynel, A., Gorse, L., Curti, C., Schafer, J., Grosbois, C., Morelli, G., Ducassou, E., Blanc, G., Maillet,
537 G.M., Mojtahid, M., 2016. Spatial distribution of trace elements in the surface sediments of a
538 major European estuary (Loire Estuary, France): Source identification and evaluation of
539 anthropogenic contribution. *Journal of Sea Research* 118, 77–91.
540 <https://doi.org/10.1016/j.seares.2016.08.005>
- 541 Dang, D.H., Lenoble, V., Durrieu, G., Omanović, D., Mullot, J.-U., Mounier, S., Garnier, C., 2015a.
542 Seasonal variations of coastal sedimentary trace metals cycling: Insight on the effect of
543 manganese and iron (oxy)hydroxides, sulphide and organic matter. *Marine Pollution Bulletin*
544 92, 113–124. <https://doi.org/10.1016/j.marpolbul.2014.12.048>
- 545 Dang, D.H., Schäfer, J., Brach-Papa, C., Lenoble, V., Durrieu, G., Dutruch, L., Chiffolleau, J.-F.,
546 Gonzalez, J.-L., Blanc, G., Mullot, J.-U., Mounier, S., Garnier, C., 2015b. Evidencing the
547 Impact of Coastal Contaminated Sediments on Mussels Through Pb Stable Isotopes
548 Composition. *Environ. Sci. Technol.* 49, 11438–11448. <https://doi.org/10.1021/acs.est.5b01893>

- 549 de Souza Machado, A.A., Spencer, K., Kloas, W., Toffolon, M., Zarfl, C., 2016. Metal fate and effects
550 in estuaries: A review and conceptual model for better understanding of toxicity. *Science of The*
551 *Total Environment* 541, 268–281. <https://doi.org/10.1016/j.scitotenv.2015.09.045>
- 552 Desaulty, A.-M., Petelet-Giraud, E., 2020. Zinc isotope composition as a tool for tracing sources and
553 fate of metal contaminants in rivers. *Science of The Total Environment* 728, 138599.
554 <https://doi.org/10.1016/j.scitotenv.2020.138599>
- 555 Druce, M., Stirling, C.H., Rolison, J.M., 2020. High-Precision Zinc Isotopic Measurement of Certified
556 Reference Materials Relevant to the Environmental, Earth, Planetary and Biomedical Sciences.
557 *Geostandards and Geoanalytical Research* 44, 711–732. <https://doi.org/10.1111/ggr.12341>
- 558 Dulaquais, G., Waeles, M., Breitenstein, J., Knoery, J., Riso, R., 2020. Links between size fractionation,
559 chemical speciation of dissolved copper and chemical speciation of dissolved organic matter in
560 the Loire estuary. *Environ. Chem.* 17, 385. <https://doi.org/10.1071/EN19137>
- 561 FAO, 2024. The European market for mussels [WWW Document]. URL [https://www.fao.org/in-](https://www.fao.org/in-action/globefish/fishery-information/resource-detail/es/c/338588/)
562 [action/globefish/fishery-information/resource-detail/es/c/338588/](https://www.fao.org/in-action/globefish/fishery-information/resource-detail/es/c/338588/) (accessed 2.2.24).
- 563 Goldberg, E.D., 1975. The mussel watch — A first step in global marine monitoring. *Marine Pollution*
564 *Bulletin* 6, 111. [https://doi.org/10.1016/0025-326X\(75\)90271-4](https://doi.org/10.1016/0025-326X(75)90271-4)
- 565 Gosling, E.M., 2015. *Marine bivalve molluscs*, Second edition. ed. Wiley Blackwell, Chichester, West
566 Sussex, UK ; Hoboken, NJ, USA.
- 567 Grasset, D., 2011. Histoire d'une tragédie navale Le sabordage de la flotte française Toulon- 27
568 novembre 194.
- 569 Grosbois, C., Meybeck, M., Lestel, L., Lefèvre, I., Moatar, F., 2012. Severe and contrasted polymetallic
570 contamination patterns (1900–2009) in the Loire River sediments (France). *Science of The Total*
571 *Environment* 435–436, 290–305. <https://doi.org/10.1016/j.scitotenv.2012.06.056>
- 572 Grouhel, A., 2023. Prescriptions techniques pour l'échantillonnage de mollusques du réseau national
573 d'observation des contaminants chimiques (ROCCH).
- 574 Hendry, K.R., Andersen, M.B., 2013. The zinc isotopic composition of siliceous marine sponges:
575 Investigating nature's sediment traps. *Chemical Geology* 354, 33–41.
576 <https://doi.org/10.1016/j.chemgeo.2013.06.025>
- 577 Jalón-Rojas, I., Schmidt, S., Sottolichio, A., Bertier, C., 2016. Tracking the turbidity maximum zone in
578 the Loire Estuary (France) based on a long-term, high-resolution and high-frequency monitoring
579 network. *Continental Shelf Research* 117, 1–11. <https://doi.org/10.1016/j.csr.2016.01.017>
- 580 Jaouen, K., Colleter, R., Pietrzak, A., Pons, M.-L., Clavel, B., Telmon, N., Crubézy, É., Hublin, J.-J.,
581 Richards, M.P., 2018. Tracing intensive fish and meat consumption using Zn isotope ratios:
582 evidence from a historical Breton population (Rennes, France). *Sci Rep* 8, 5077.
583 <https://doi.org/10.1038/s41598-018-23249-x>
- 584 Jeong, H., Ra, K., Choi, J.Y., 2021a. Copper, Zinc and Lead Isotopic Delta Values and Isotope Ratios
585 of Various Geological and Biological Reference Materials. *Geostandards and Geoanalytical*
586 *Research* 45, 551–563. <https://doi.org/10.1111/ggr.12379>
- 587 Jeong, H., Ra, K., Won, J.-H., 2021b. A nationwide survey of trace metals and Zn isotopic signatures in
588 mussels (*Mytilus edulis*) and oysters (*Crassostrea gigas*) from the coast of South Korea. *Marine*
589 *Pollution Bulletin* 173, 113061. <https://doi.org/10.1016/j.marpolbul.2021.113061>
- 590 John, S.G., Genevieve Park, J., Zhang, Z., Boyle, E.A., 2007. The isotopic composition of some common
591 forms of anthropogenic zinc. *Chemical Geology* 245, 61–69.
592 <https://doi.org/10.1016/j.chemgeo.2007.07.024>
- 593 Juillot, F., Noël, V., Louvat, P., Gelabert, A., Jouvin, D., Göttlicher, J., Belin, S., Müller, B., Morin, G.,
594 Voegelin, A., 2023. Can Zn isotopes in sediments record past eutrophication of freshwater
595 lakes? A pilot study at Lake Baldegg (Switzerland). *Chemical Geology* 620, 121321.
596 <https://doi.org/10.1016/j.chemgeo.2023.121321>
- 597 Kersten, M., Smedes, F., 2002. Normalization procedures for sediment contaminants in spatial and
598 temporal trend monitoring. *J. Environ. Monit.* 4, 109–115. <https://doi.org/10.1039/B108102K>
- 599 Köbberich, M., Vance, D., 2019. Zn isotope fractionation during uptake into marine phytoplankton:
600 Implications for oceanic zinc isotopes. *Chemical Geology* 523, 154–161.
601 <https://doi.org/10.1016/j.chemgeo.2019.04.004>
- 602 Komárek, M., Ratié, G., Vaňková, Z., Šípková, A., Chrastný, V., 2021. Metal isotope complexation with
603 environmentally relevant surfaces: Opening the isotope fractionation black box. *Critical*
604 *Reviews in Environmental Science and Technology* 0, 1–31.
605 <https://doi.org/10.1080/10643389.2021.1955601>

- 606 Krishnakumar, P.K., Qurban, M.A., Sasikumar, G., 2018. Biomonitoring of Trace Metals in the Coastal
607 Waters Using Bivalve Molluscs, in: Saleh, H.E.-D.M., El-Adham, E. (Eds.), Trace Elements -
608 Human Health and Environment. InTech. <https://doi.org/10.5772/intechopen.76938>
- 609 Latouche, D., Mix, M.C., 1981. Seasonal variation in soft tissue weights and trace metal burdens in the
610 bay mussel, *Mytilus edulis*. *Bulletin of Environmental Contamination and Toxicology* 27, 821–
611 828.
- 612 Little, S.H., Archer, C., Milne, A., Schlosser, C., Achterberg, E.P., Lohan, M.C., Vance, D., 2018. Paired
613 dissolved and particulate phase Cu isotope distributions in the South Atlantic. *Chemical*
614 *Geology* 502, 29–43. <https://doi.org/10.1016/j.chemgeo.2018.07.022>
- 615 Little, S.H., Vance, D., McManus, J., Severmann, S., 2016. Key role of continental margin sediments in
616 the oceanic mass balance of Zn and Zn isotopes. *Geology* 44, 207–210.
617 <https://doi.org/10.1130/G37493.1>
- 618 Little, S.H., Vance, D., Walker-Brown, C., Landing, W.M., 2014. The oceanic mass balance of copper
619 and zinc isotopes, investigated by analysis of their inputs, and outputs to ferromanganese oxide
620 sediments. *Geochimica et Cosmochimica Acta* 125, 673–693.
621 <https://doi.org/10.1016/j.gca.2013.07.046>
- 622 Little, S.H., Wilson, D.J., Rehkämper, M., Adkins, J.F., Robinson, L.F., van de Fliedert, T., 2021. Cold-
623 water corals as archives of seawater Zn and Cu isotopes. *Chemical Geology* 578, 120304.
624 <https://doi.org/10.1016/j.chemgeo.2021.120304>
- 625 Liu, Y., Chen, M., Zhang, T., Zhang, R., Cao, F., Sun, S., Zheng, W., Sun, R., Chen, J., 2023. Isotope
626 Compositions of Century-Long Corals Reveal Significant Dissolved Cu, Zn Fluxes From
627 Human-Accelerated Weathering Into the Ocean. *Geophysical Research Letters* 50,
628 e2022GL102482. <https://doi.org/10.1029/2022GL102482>
- 629 Lobel, P.B., Wright, D.A., 1982. Gonadal and Nongonadal Zinc Concentrations in Mussels. *Marine*
630 *Pollution Bulletin* 13, 320–323.
- 631 Lu, G., Pan, K., Zhu, A., Dong, Y., Wang, W.-X., 2020. Spatial-temporal variations and trends
632 predication of trace metals in oysters from the Pearl River Estuary of China during 2011–2018.
633 *Environmental Pollution* 264, 114812. <https://doi.org/10.1016/j.envpol.2020.114812>
- 634 Lu, G.-Y., Wang, W.-X., 2018. Trace metals and macroelements in mussels from Chinese coastal
635 waters: National spatial patterns and normalization. *Science of The Total Environment* 626,
636 307–318. <https://doi.org/10.1016/j.scitotenv.2018.01.018>
- 637 Ma, L., Li, Y., Wang, W., Weng, N., Evans, R.D., Wang, W.-X., 2019. Zn Isotope Fractionation in the
638 Oyster *Crassostrea hongkongensis* and Implications for Contaminant Source Tracking.
639 *Environ. Sci. Technol.* 53, 6402–6409. <https://doi.org/10.1021/acs.est.8b06855>
- 640 Ma, L., Wang, W.-X., Evans, R.D., 2021. Distinguishing multiple Zn sources in oysters in a complex
641 estuarine system using Zn isotope ratio signatures. *Environmental Pollution* 289, 117941.
642 <https://doi.org/10.1016/j.envpol.2021.117941>
- 643 McCormack, J., Szpak, P., Bourgon, N., Richards, M., Hyland, C., Méjean, P., Hublin, J.-J., Jaouen, K.,
644 2021. Zinc isotopes from archaeological bones provide reliable trophic level information for
645 marine mammals. *Commun Biol* 4, 683. <https://doi.org/10.1038/s42003-021-02212-z>
- 646 Moynier, F., Borgne, M.L., Lahoud, E., Mahan, B., Mouton-Liger, F., Hugon, J., Paquet, C., 2020.
647 Copper and zinc isotopic excursions in the human brain affected by Alzheimer's disease.
648 *Alzheimer's & Dementia: Diagnosis, Assessment & Disease Monitoring* 12, e12112.
649 <https://doi.org/10.1002/dad2.12112>
- 650 Moynier, F., Vance, D., Fujii, T., Savage, P., 2017. The Isotope Geochemistry of Zinc and Copper.
651 *Reviews in Mineralogy and Geochemistry* 82, 543–600.
652 <https://doi.org/10.2138/rmg.2017.82.13>
- 653 Nicolau, R., Lucas, Y., Merdy, P., Raynaud, M., 2012. Base flow and stormwater net fluxes of carbon
654 and trace metals to the Mediterranean sea by an urbanized small river. *Water Research, Special*
655 *Issue on Stormwater in urban areas* 46, 6625–6637.
656 <https://doi.org/10.1016/j.watres.2012.01.031>
- 657 OSPAR, 2018. CEMP guidelines for monitoring contaminants in sediments. Revised in 2018.
658 Agreement 2002-16. <https://www.ospar.org/documents?d=32743>.
- 659 Oursel, B., Garnier, C., Zebracki, M., Durrieu, G., Pairaud, I., Omanović, D., Cossa, D., Lucas, Y., 2014.
660 Flood inputs in a Mediterranean coastal zone impacted by a large urban area: Dynamic and fate
661 of trace metals. *Marine Chemistry, Estuarine Biogeochemistry* 167, 44–56.
662 <https://doi.org/10.1016/j.marchem.2014.08.005>

- 663 Pougnet, F., Schäfer, J., Dutruch, L., Garnier, C., Tessier, E., Dang, D.H., Lanceleur, L., Mullot, J.-U.,
664 Lenoble, V., Blanc, G., 2014. Sources and historical record of tin and butyl-tin species in a
665 Mediterranean bay (Toulon Bay, France). *Environ Sci Pollut Res* 21, 6640–6651.
666 <https://doi.org/10.1007/s11356-014-2576-6>
- 667 Rainbow, P.S., 2007. Trace metal bioaccumulation: Models, metabolic availability and toxicity.
668 *Environment International* 33, 576–582. <https://doi.org/10.1016/j.envint.2006.05.007>
- 669 Rodríguez-Rodríguez, G., Bande Ramudo, R., 2017. Market driven management of climate change
670 impacts in the Spanish mussel sector. *Marine Policy* 83, 230–235.
671 <https://doi.org/10.1016/j.marpol.2017.06.014>
- 672 Schilling, K., Harris, A.L., Halliday, A.N., Schofield, C.J., Sheldon, H., Haider, S., Lerner, F., 2021.
673 Investigations on Zinc Isotope Fractionation in Breast Cancer Tissue Using in vitro Cell Culture
674 Uptake-Efflux Experiments. *Front Med (Lausanne)* 8, 746532.
675 <https://doi.org/10.3389/fmed.2021.746532>
- 676 Schlacher-Hoenlinger, M.A., Schlacher, T.A., 1998. Accumulation, contamination, and seasonal
677 variability of trace metals in the coastal zone – patterns in a seagrass meadow from the
678 Mediterranean. *Marine Biology* 131, 401–410. <https://doi.org/10.1007/s002270050333>
- 679 Sen, I.S., Peucker-Ehrenbrink, B., 2012. Anthropogenic Disturbance of Element Cycles at the Earth's
680 Surface. *Environ. Sci. Technol.* 46, 8601–8609. <https://doi.org/10.1021/es301261x>
- 681 Shiel, A.E., Weis, D., Cossa, D., Orians, K.J., 2013. Determining provenance of marine metal pollution
682 in French bivalves using Cd, Zn and Pb isotopes. *Geochimica et Cosmochimica Acta* 121, 155–
683 167. <https://doi.org/10.1016/j.gca.2013.07.005>
- 684 Shiel, A.E., Weis, D., Orians, K.J., 2012. Tracing cadmium, zinc and lead sources in bivalves from the
685 coasts of western Canada and the USA using isotopes. *Geochim. Cosmochim. Acta* 76, 175–
686 190. <https://doi.org/10.1016/j.gca.2011.10.005>
- 687 Soto, M., Ireland, M.P., Marigómez, I., 2000. Changes in mussel biometry on exposure to metals:
688 implications in estimation of metal bioavailability in 'Mussel-Watch' programmes. *Science of The Total Environment* 247, 175–187. [https://doi.org/10.1016/S0048-9697\(99\)00489-1](https://doi.org/10.1016/S0048-9697(99)00489-1)
- 690 Sullivan, K.V., Kidder, J.A., Junqueira, T.P., Vanhaecke, F., Leybourne, M.I., 2022. Emerging
691 applications of high-precision Cu isotopic analysis by MC-ICP-MS. *Science of The Total Environment* 838, 156084. <https://doi.org/10.1016/j.scitotenv.2022.156084>
- 693 Tessier, E., Garnier, C., Mullot, J.-U., Lenoble, V., Arnaud, M., Raynaud, M., Mounier, S., 2011. Study
694 of the spatial and historical distribution of sediment inorganic contamination in the Toulon bay
695 (France). *Marine Pollution Bulletin* 62, 2075–2086.
696 <https://doi.org/10.1016/j.marpolbul.2011.07.022>
- 697 Thibon, Fanny, Metian, M., Oberhänsli, F., Montanes, M., Vassileva, E., Orani, A.M., Telouk, P.,
698 Swarzenski, P., Vigier, N., 2021. Bioaccumulation of Lithium Isotopes in Mussel Soft Tissues
699 and Implications for Coastal Environments. *ACS Earth Space Chem.* 5, 1407–1417.
700 <https://doi.org/10.1021/acsearthspacechem.1c00045>
- 701 Thibon, F., Weppe, L., Vigier, N., Churlaud, C., Lacoue-Labarthe, T., Metian, M., Cherel, Y.,
702 Bustamante, P., 2021. Large-scale survey of lithium concentrations in marine organisms.
703 *Science of The Total Environment* 751, 141453.
704 <https://doi.org/10.1016/j.scitotenv.2020.141453>
- 705 Toubhans, B., Gourlan, A.T., Telouk, P., Lutchman-Singh, K., Francis, L.W., Conlan, R.S., Margarit,
706 L., Gonzalez, D., Charlet, L., 2020. Cu isotope ratios are meaningful in ovarian cancer
707 diagnosis. *Journal of Trace Elements in Medicine and Biology* 62, 126611.
708 <https://doi.org/10.1016/j.jtemb.2020.126611>
- 709 Waeles, M., Riso, R.D., Maguer, J.-F., Le Corre, P., 2004. Distribution and chemical speciation of
710 dissolved cadmium and copper in the Loire estuary and North Biscay continental shelf, France.
711 *Estuarine, Coastal and Shelf Science* 59, 49–57. <https://doi.org/10.1016/j.ecss.2003.07.009>
- 712 Wang, L., Wang, X., Chen, H., Wang, Z., Jia, X., 2022. Oyster arsenic, cadmium, copper, mercury, lead
713 and zinc levels in the northern South China Sea: long-term spatiotemporal distributions,
714 combined effects, and risk assessment to human health. *Environ Sci Pollut Res* 29, 12706–
715 12719. <https://doi.org/10.1007/s11356-021-18150-6>
- 716 Wang, Z., Kwon, K.D., Peacock, C., Mo, X., Gou, W., Feng, X., Li, W., 2022. Zn stable isotope
717 fractionation during adsorption onto todorokite: A molecular perspective from X-ray absorption
718 spectroscopy and density functional theory. *Geochimica et Cosmochimica Acta* 327, 116–136.
719 <https://doi.org/10.1016/j.gca.2022.04.016>

- 720 Wiederhold, J.G., 2015. Metal Stable Isotope Signatures as Tracers in Environmental Geochemistry.
721 Environ. Sci. Technol. 49, 2606–2624. <https://doi.org/10.1021/es504683e>
- 722 Wijsman, J.W.M., Troost, K., Fang, J., Roncarati, A., 2019. Global Production of Marine Bivalves.
723 Trends and Challenges, in: Smaal, A.C., Ferreira, J.G., Grant, J., Petersen, J.K., Strand, Ø.
724 (Eds.), Goods and Services of Marine Bivalves. Springer International Publishing, Cham, pp.
725 7–26. https://doi.org/10.1007/978-3-319-96776-9_2
- 726 Xiao, H., Deng, W., Wei, G., Chen, J., Zheng, X., Shi, T., Chen, X., Wang, C., Liu, X., Zeng, T., 2020.
727 A Pilot Study on Zinc Isotopic Compositions in Shallow-Water Coral Skeletons. Geochemistry,
728 Geophysics, Geosystems 21, e2020GC009430. <https://doi.org/10.1029/2020GC009430>
- 729 Zhang, R., Russell, J., Xiao, X., Zhang, F., Li, T., Liu, Z., Guan, M., Han, Q., Shen, L., Shu, Y., 2018.
730 Historical records, distributions and sources of mercury and zinc in sediments of East China
731 sea: Implication from stable isotopic compositions. Chemosphere 205, 698–708.
732 <https://doi.org/10.1016/j.chemosphere.2018.04.100>
- 733 Zhang, T., Sun, R., Liu, Y., Chen, L., Zheng, W., Liu, C.-Q., Chen, J., 2022. Copper and Zinc isotope
734 signatures in scleratinian corals: Implications for Cu and Zn cycling in modern and ancient
735 ocean. Geochimica et Cosmochimica Acta 317, 395–408.
736 <https://doi.org/10.1016/j.gca.2021.10.014>
737
- 738
- 739
- 740

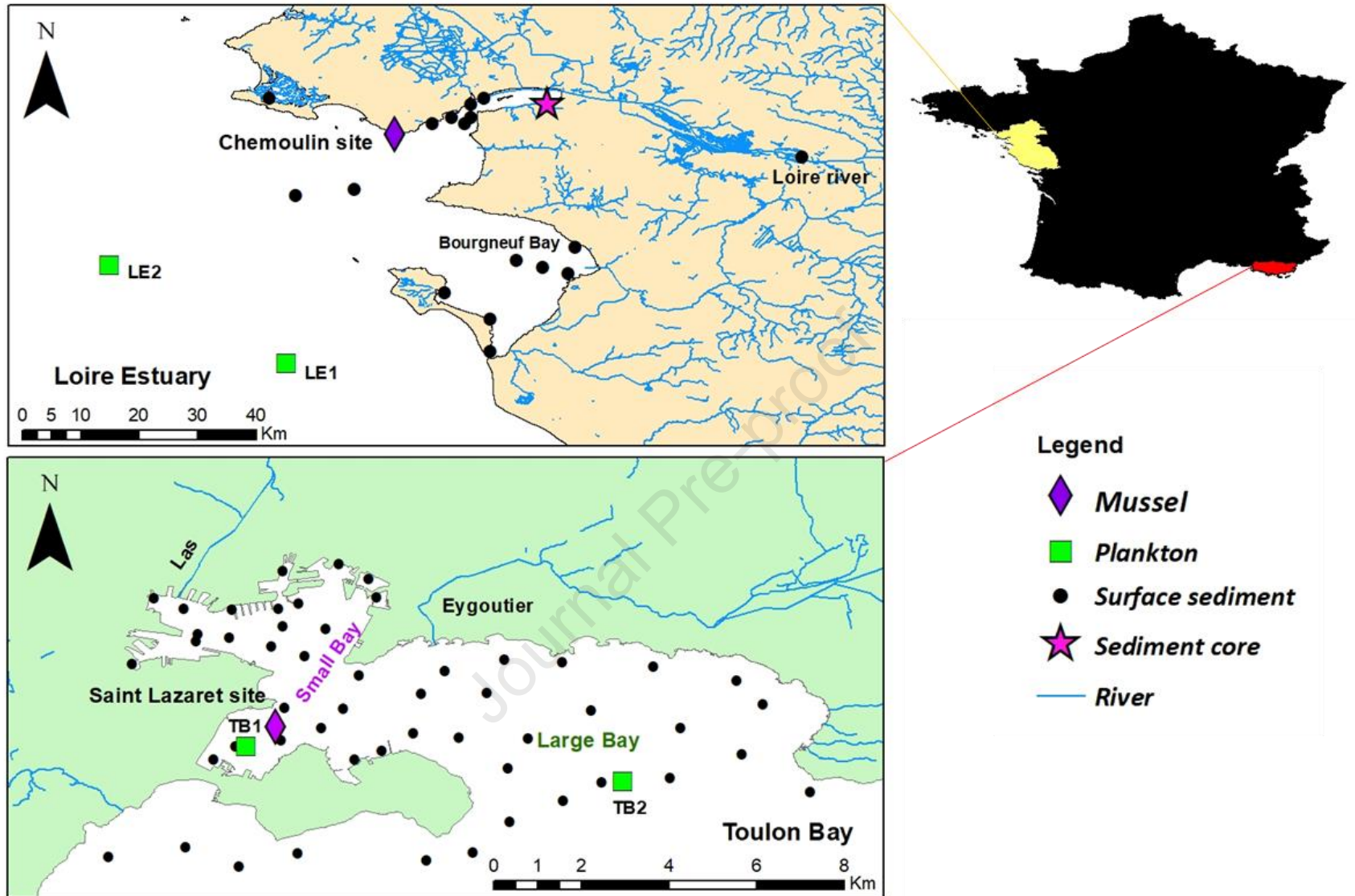


Fig. 1. Geographic distribution of sampling stations: mussel stations (rhombus symbols) are positioned at the Chemoulin site (Loire Estuary) and the Saint Lazaret site (Toulon Bay).

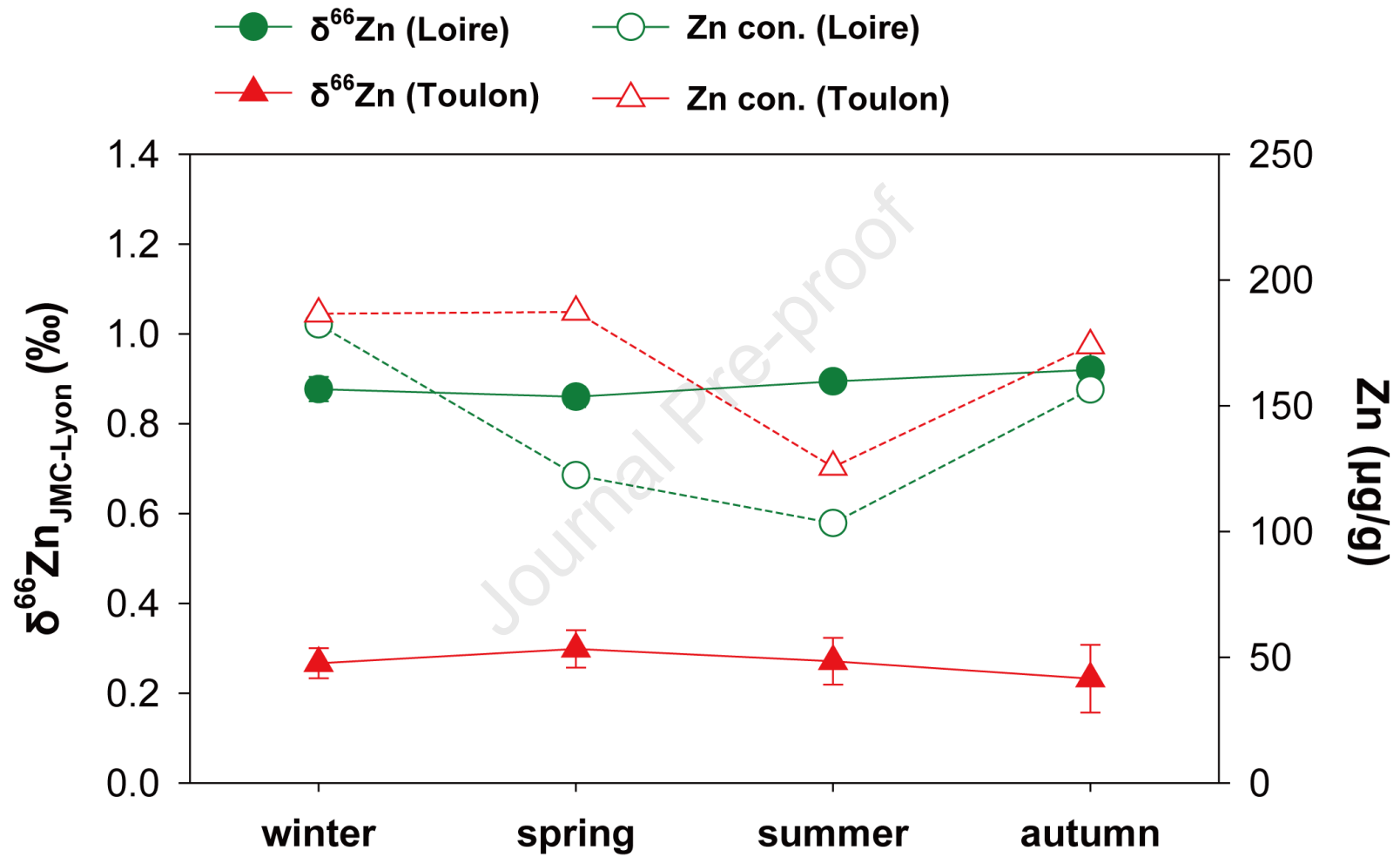


Fig. 2. Seasonal elemental and isotope variations in zinc (Zn) in mussels.

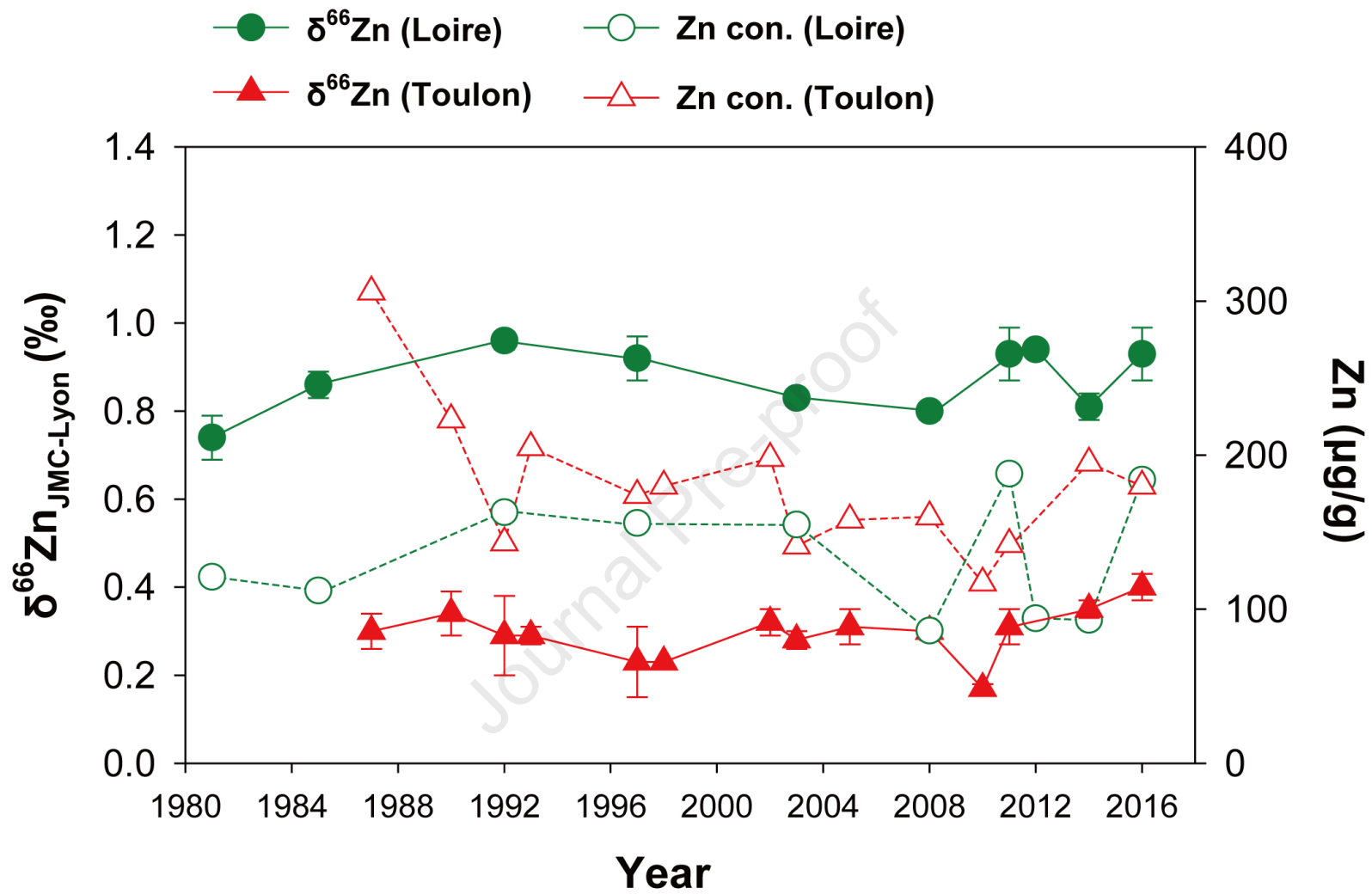


Fig. 3. Elemental and isotope variations in zinc (Zn) in mussels over decades.

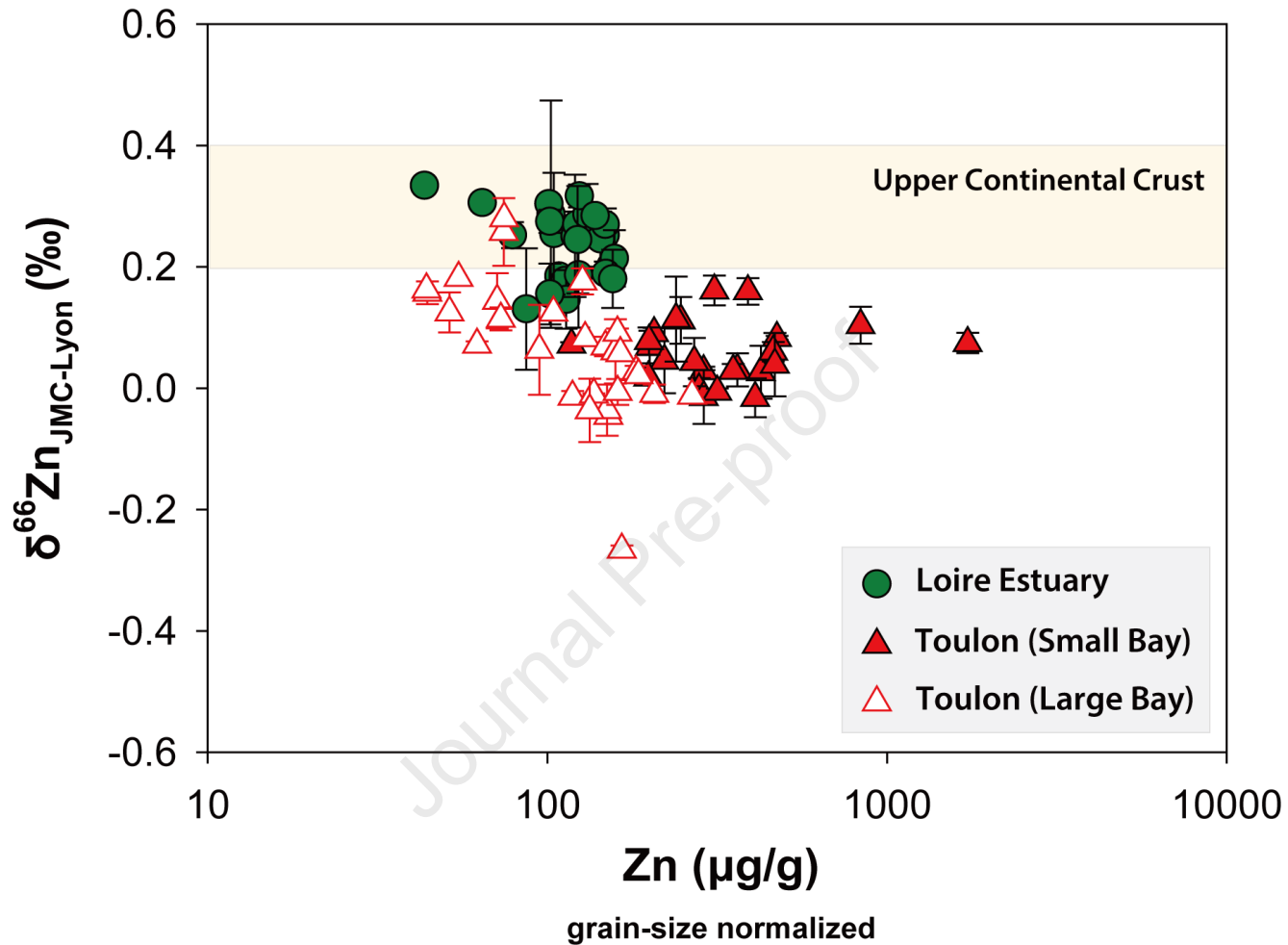


Fig. 4. Zinc (Zn) elemental and isotope data of Loire Estuary and Toulon Bay sediments. The Zn concentrations are normalized to grain size using an aluminum (Al) content of 5% and are displayed on a logarithmic scale. The Upper Continental Crust (UCC) correspond to the approximate average range reported in the literature (Moynier et al., 2017).

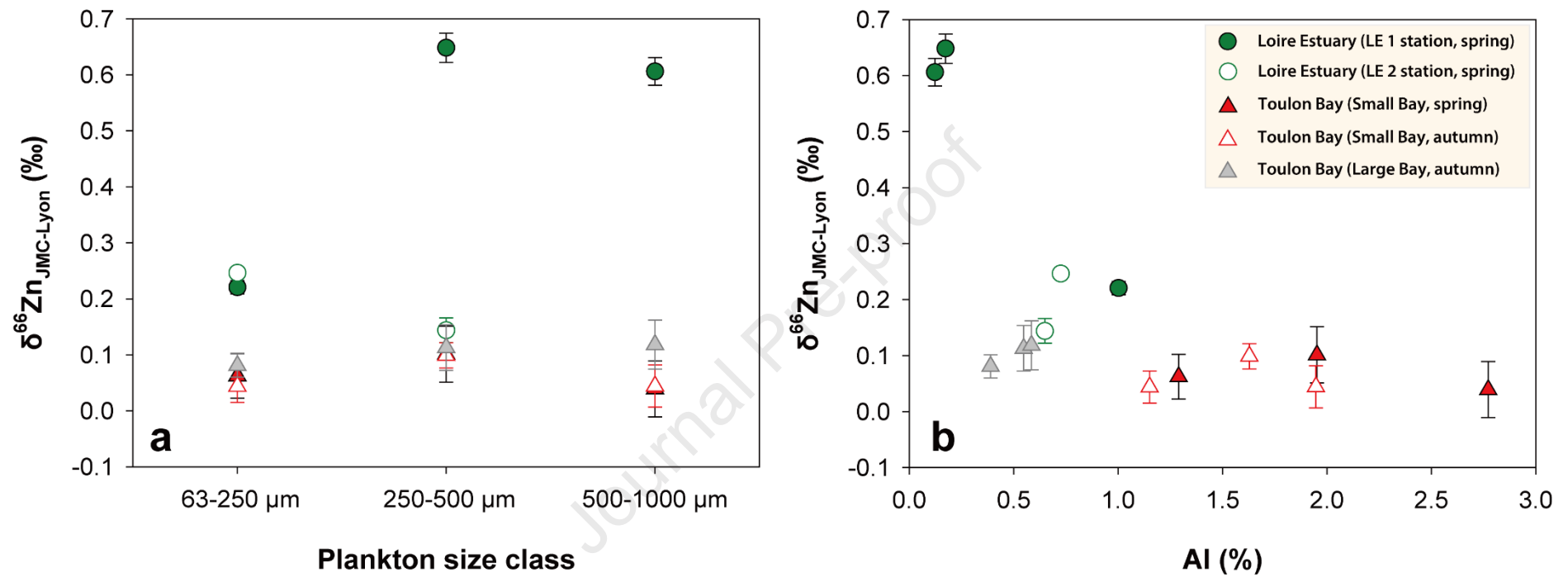


Fig. 5. Zinc (Zn) isotope compositions of plankton samples. a) $\delta^{66}\text{Zn}$ values for the different plankton size classes; (b) scatter plot of $\delta^{66}\text{Zn}$ vs. aluminum (Al).

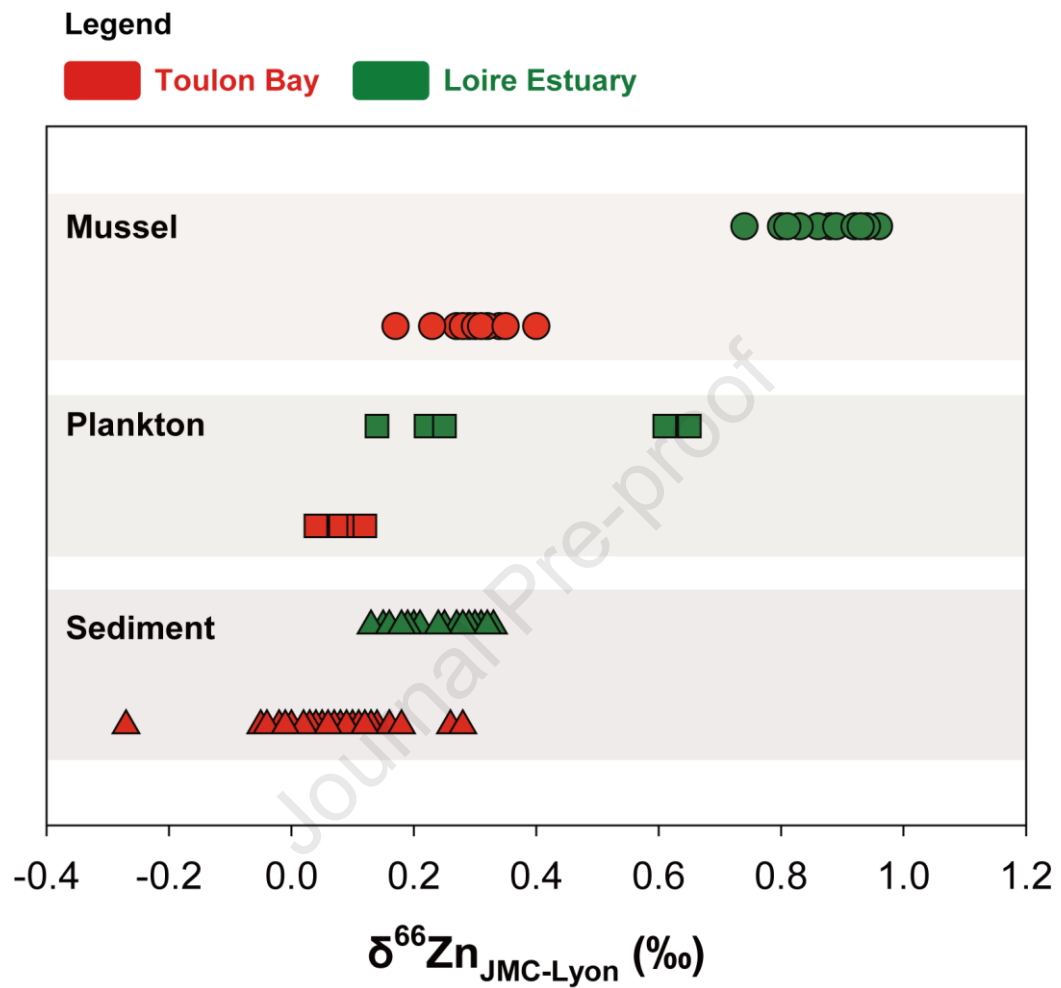


Fig. 6. Multi-compartment zinc (Zn) isotope compositions from the Loire Estuary and Toulon Bay.

Table 1. Isotope compositions of reference materials (RM)s reported against the "JMC-Lyon" standard. The "*n*" refers to number of distinct aliquots proceed through all procedure. Each aliquot was analysed twice or thrice.

Matrix	Reference material	$\delta^{66}\text{Zn}$ (this study)	$\delta^{66}\text{Zn}$ (Literature)	authors
Oyster	SRM 1566b	0.70 ± 0.05 ($n = 5$)	0.71 ± 0.02 ($n = 4$)	Jeong et al., 2021
Mussel	ERM-CE278K	0.41 ± 0.05 ($n = 3$)	0.56 ± 0.04 ($n = 4$)	Jeong et al., 2021
Sediment	MESS-3	0.26 ± 0.06 ($n = 10$)	0.28 ± 0.02 ($n = 13$)	Druce et al., 2020
Plankton	BCR 414	0.23 ± 0.09 ($n = 1$)	0.29 ± 0.04 ($n = 4$)	Jeong et al., 2021

Table 2. Summary of elemental and isotope datasets of zinc used in this study.

Site	Matrix	Sampling date	Reference	Table
Loire Estuary	Surface sediment/Sediment core	2014 and 2015	<u>Araújo et al., 2019b</u>	S3
	Plankton	2013	Araújo et al., 2022a	S1
	Mussel	From 1981 to 2016	This study	S4
Toulon Bay	Surface sediment	2008 and 2009	<u>Araújo et al., 2019a</u>	S2
	Plankton	2018	This study	S1
	Mussel	From 1987 to 2016	This study	S4

Highlights

- Pristine and contaminated sites show samples with distinct isotope fingerprints.
- Systematic lighter $\delta^{66}\text{Zn}$ values identify anthropogenic Zn in contaminated samples.
- Zn isotopes trace upward transfer of anthropogenic Zn in the food web.
- Isotope biomonitors indicate no alterations in Zn sources over four decades.
- Zn isotope ratio constancy at seasonal scale discards biological isotope effects.

Journal Pre-proof

All authors have approved the submission of this manuscript, and we collectively affirm that the content of the manuscript is original and has not been published or is currently under consideration elsewhere.

Journal Pre-proof